

# Vegetation dynamics and its response to climate change during the past 2000 years in the Altai Mountains, northwestern China

Dongliang ZHANG (✉)<sup>1,2,3,4</sup>, Yunpeng YANG<sup>5,6</sup>, Min RAN<sup>5,6</sup>, Bo LAN<sup>7</sup>, Hongyan ZHAO<sup>8</sup>, Qi LIU<sup>9</sup>

1 State Key Laboratory of Desert and Oasis Ecology, Xinjiang Institute of Ecology and Geography, Chinese Academy of Sciences, Urumqi 830011, China

2 Research Center for Ecology and Environment of Central Asia, Chinese Academy of Sciences, Urumqi 830011, China.

3 University of Chinese Academy of Sciences, Beijing 100049, China

4 State Key Laboratory of Loess and Quaternary Geology, Institute of Earth Environment, Chinese Academy of Sciences, Xi'an 710061, China

5 College of Environment and Planning, Henan University, Kaifeng 475004, China

6 Key Laboratory of Geospatial Technology for the Middle and Lower Yellow River Regions (Ministry of Education), Henan University, Kaifeng 475004, China

7 School of Environmental and Chemical Engineering, Chongqing Three Gorges University, Chongqing 404000, China

8 School of Earth Science, Northeast Normal University, Changchun 130024, China

9 College of Resource and Environmental Sciences, Xinjiang University, Urumqi 830046, China

© Higher Education Press 2021

**Abstract** Over the past 2000 years, a high-resolution pollen record from the Yushenkule Peat (46°45′–46°57′N, 90°46′–90°61′E, 2374 m a.s.l.) in the south-eastern Altai Mountains of northwestern China has been used to explore the changes in vegetation and climate. The regional vegetation has been dominated by alpine meadows revealed from pollen diagrams over the past 2000 years. The pollen-based climate was warm and wet during the Roman Warm Period (0–520 AD), cold and wet during the Dark Age Cold Period (520–900 AD), warm and wet during the Medieval Warm Period (900–1300 AD), and cold and dry during the Little Ice Age (1300–1850 AD). Combined with other pollen data from the Altai Mountains, we found that the percentage of arboreal pollen showed a reduced trend along the NW-SE gradient with decreasing moisture and increasing climatic continentality of the Altai Mountains over the past 2000 years; this is consistent with modern distributions of taiga forests. We also found that the taiga (*Pinus* forest) have spread slightly, while the steppe (*Artemisia*, Poaceae and Chenopodiaceae) have recovered significantly in the Altai Mountains over the past 2000 years. In addition, the relatively warm-wet climate may promote high grassland productivity and southward expansion of steppe, which favors the formation of Mongol political and military power.

**Keywords** pollen analysis, vegetation dynamics, past 2000 years, Altai mountains, northwestern China

## 1 Introduction

The Altai Mountains, stretching over China, Kazakhstan, Russia and Mongolia, have been regarded as the boundary between the Asian monsoon-affected eastern Central Asia and the westerlies-influenced western Central Asia (Blyakharchuk et al., 2007, 2008; Feng et al., 2017; Rudaya et al., 2009). As an important divide between the desert steppes in the south and the Siberian taiga forests in the north, the Altai Mountains are an ideal region for uncovering past vegetation dynamics and climate changes (Blyakharchuk and Chernova, 2013; Huang et al., 2018).

Holocene vegetation dynamics and associated climate changes in the Altai Mountains have been intensively investigated (e.g., Rudaya et al., 2009; Feng et al., 2017; Huang et al., 2018; Wang and Zhang, 2019; Zhang et al., 2020a, 2020b). For example, pollen data from Kanas Lake indicate that the forest optimum occurred at ~10–7 cal. kyr BP and that the progressive opening of the forest was caused by the climatic cooling since ~7 cal. kyr BP (Huang et al., 2018). The pollen records of the nearby Narenxia Peatland revealed the expansion of taiga forests before ~7 cal. kyr BP, the development of steppe at the expense of the taiga forest during ~7–3.2 cal. kyr BP, and again the recovery of the taiga forest after ~3.2 cal. kyr BP (Feng

et al., 2017). Moreover, the slightly increased taiga biome scores in the late Holocene were also observed in the Tuolehte Peatland (Zhang et al., 2020a). The obvious differences in the late-Holocene vegetation evolution have impeded our understanding of the relationship between vegetation and climate changes in the Altai Mountains.

Thus, to deeply examine the variability of the late-Holocene vegetation and climate in the Altai Mountains, first, this study reported a new pollen record inferred from the Yushenkule (YSKL) Peatland to reconstruct the vegetation and climate history of the past 2000 years in the south-eastern Altai Mountains of north-western China. Subsequently, the YSKL data was compared with the previous published high-resolution pollen data (i.e., Narenxia Peatland, Kanas Lake, Big Black Peatland, Tuolehaite Peatland, and Halasazi Peatland) of the whole Altai Mountains. The objectives of this study were (i) to reveal the past 2000-year variations of vegetation and climate in the south-eastern Altai Mountains, and (ii) to investigate the vegetation dynamics of the past 2000 years in the Altai Mountains.

## 2 Materials and methods

### 2.1 Study area and field sampling

The Altai Mountains begin from the Southern Siberian Plains in Russia and terminate at the Gobi Desert in Mongolia (Fig. 1(a)). They are characterized by north-west-south-east (NW-SE) gradients of decreasing elevation and precipitation. The vegetation well reflects the decreasing precipitation gradients in the Altai Mountains. Dark coniferous forests with *Abies sibirica*, *Picea obovata* and *Pinus sibirica* occupy the north-western Altai Mountains, and light coniferous forests (i.e., *Larix*

*sibirica*) and herb communities overlay the south-eastern parts (Borisov, 1957; Milkov and Gvozdezky, 1996; Blyakharchuk et al., 2004). The desert steppes dominate the leeward/sunny slopes and intermountain basins of the Gobi Desert in Mongolia (Borisov, 1957; Blyakharchuk et al., 2004, 2007).

The regional climate is temperate continental with a cold-dry winter from October to April and a warm-wet summer from May to September. The mean annual temperature (MAT) ranges from  $-2^{\circ}\text{C}$  to  $3^{\circ}\text{C}$ , and the mean annual precipitation (MAP) amounts to 250 to 450 mm, with  $>80\%$  occurring from May to September (Zhang et al., 2018). From 1970 to 2015, the Altai Mountains had a rapidly warming trend at a rate of  $0.41^{\circ}\text{C}/\text{decade}$ , and an insignificant wetting trend at a rate of  $4.82\text{ mm}/\text{decade}$  (Li et al., 2020).

The selected YSKL Peatland ( $46^{\circ}45'–46^{\circ}57'\text{N}$ ,  $90^{\circ}46'–90^{\circ}61'\text{E}$ , 2374 m a.s.l.) is a subalpine bog, encompassing 1180  $\text{hm}^2$  in a U-shaped valley (Figs. 1(b) and 1(c)). The vegetation mainly consists of *Festuca kryloviana*, *Saussurea involucrate*, *Callianthemum*, and *alatavicum* (Yang et al., 2019a). The YSKL Peatland has few and scattered peat mounds; these are low and form long parallel shapes with an average height of 2 m and a diameter of 5 to 7 m (Zhang et al., 2018b). In August 2019, a thickness of 88 cm was measured at the exposed side of the largest peat mound. A stainless steel knife was used to slice the samples at 1 cm intervals of the YSKL core (length 88 cm) in the field, where the below 88 cm was the gley layer. All the samples were packed in tagged and sealed polyethylene plastic bags and subsequently taken to the laboratory for storage at  $-4^{\circ}\text{C}$  prior to analysis.

### 2.2 Stratigraphy and chronology

The YSKL core consists of non-vascular plants, such as

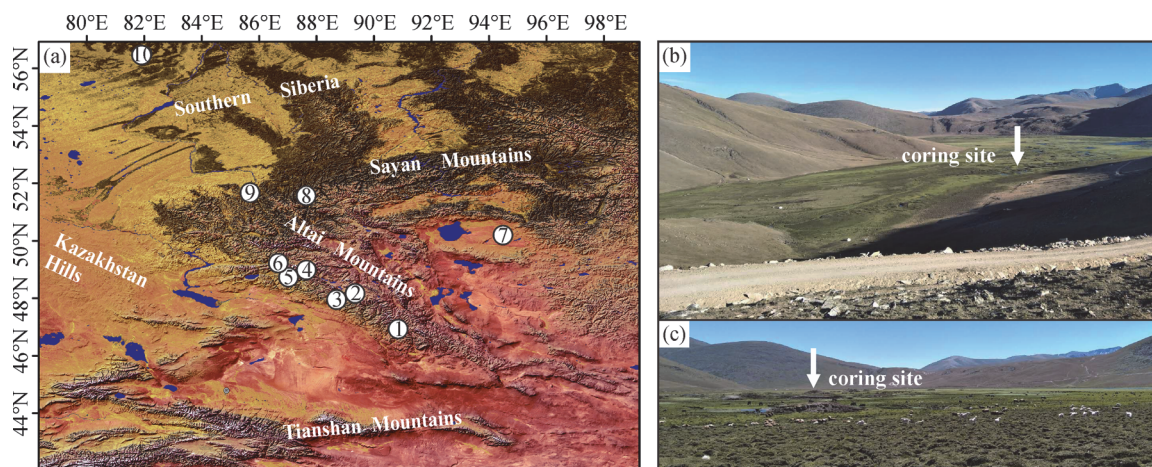


**Fig. 1** Physiographic settings of Yushenkule (YSKL) Peatland (site 1). (a) geomorphic and topographic backgrounds. The cited sites in this study include: ②—Halasazi Peatland; ③—Tuolehaite Peatland, ④—Big Black Peatland, ⑤—Kanas Lake, ⑥—Narenxia Peatland, ⑦—Bayan Nuur, ⑧—Teletskoye Lake, ⑨—Manzherok Lake and ⑩—SIB04 peat core in southern Siberian Lowland. (b) and (c) panorama of YSKL Peatland and the coring site (white vertical arrow).

*Sphagnum eymbifolium*, *Sphagnum acutifolium*, *Sphagnum teres*, and some vascular *Carex* (Yang et al., 2019a). Specifically, the upper part (1 to 10 cm) is a mixture of *Sphagnum/Carex* species, while *Sphagnum* solely prevails over the rest (11 to 88 cm). It should be noted that the samples were insufficient for a pollen analysis of the down core (88 to 84 cm). Seven samples of YSKL core were dated using AMS  $^{14}\text{C}$  radiocarbon dating at the NSF-AMS Facility of the University of Arizona. The depth-age model was constructed using the ‘Bacon’ piece-wise linear accumulation model (Blaauw, 2010) in R software (Fig. 2). The down part (83 cm) of the YSKL core dated to ~1938 cal. yr BP (i.e., 12 AD). The related laboratory numbers, testing materials and calibrated ages are showed in Table 1 (Yang et al., 2019a).

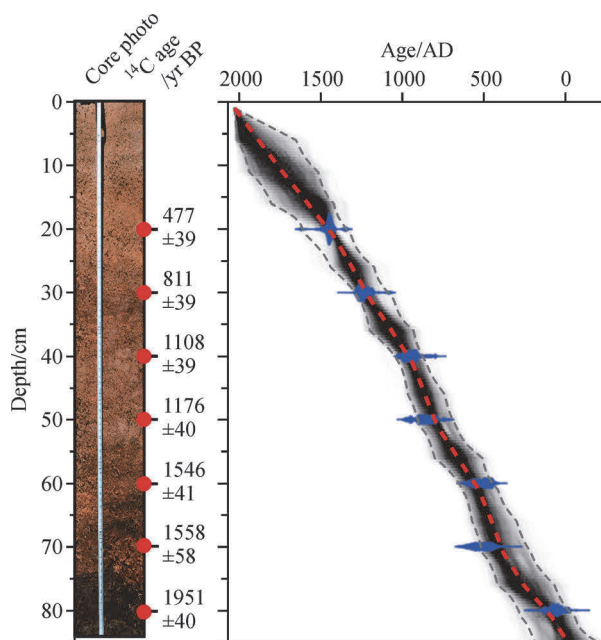


**Fig. 2** Bacon depth-age model for YSKL core (core length: 83 cm), overlaying the calibrated distributions of the individual dates (blue). Dashed lines indicate the model's 95% probability intervals. Note: the information of dates was showed in Table 1 from Yang et al. (2019a).

### 2.3 Pollen analysis

One tablet of *Lycopodium* was added to the samples for determining the pollen concentrations. The preparation of pollen samples (1 g fresh sample) in the laboratory involved treatments with hydrochloric acid (HCl, 36%, 5 mL), sodium hydroxide (NaOH, 10%, 5 mL), hydrofluoric acid (HF, 40%, 5 mL), a 9:1 mixture (3 mL) of acetic anhydride and concentrated sulfuric acid, sieving with a 10- $\mu\text{m}$  mesh screen in an ultrasonic bath, and mounting in glycerine. Subsequently, pollen identification and counting were carried out under an Olympus BX-53 light microscope with 400 times magnification, which led to the identification and counting of more than 600 terrestrial pollen grains (Wang et al., 1995) per sample of the YSKL core. The total sum of terrestrial pollen taxa was used as the denominator when calculating pollen percentages, while the percentage of fern spores was calculated based on the sum of terrestrial pollen in combination with fern spores. The pollen diagram was plotted using the Tilia 1.7.16 software.

### 2.4 Principal component analysis (PCA)

A total of 17 pollen taxa from the YSKL core were selected, and the analyses were carried out based on the square root of the transformed pollen percentage data using Canoco 4.5 (TerBraak and Smilauer, 2003). PCA was selected to analyze the pollen assemblages in the YSKL core using inter-species correlations and pollen percentages (Birks and Gordon, 1985; Han et al., 2020).

## 3 Results

### 3.1 Pollen assemblages of YSKL core

A total of 55 pollen and spore taxa were identified in 83 samples of the YSKL core, including 15 trees and 40 herbs (Fig. 3). Arboreal pollen (AP) mainly comprises *Pinus* (0.19%–1.49%), *Picea* (0.18%–1.39%), *Larix* (0.22%–1.72%) and *Betula* (0.18%–1.12%), while non-arboreal pollen (NAP) comprises Cyperaceae (21.59%–83.78%),

**Table 1** AMS  $^{14}\text{C}$  dating results of Yushenkule Peatland (reported in Yang et al. (2019a)).

LAB code	Depth/cm	Dated material	$^{14}\text{C}$ age/yr BP
AA104612	20	Plant residuals	477±39
AA104613	30	Plant residuals	811±39
AA104614	40	Plant residuals	1108±39
AA104615	50	Plant residuals	1176±40
AA104616	60	Plant residuals	1546±41
AA104617	70	Plant residuals	1558±58
AA104618	80	Plant residuals	1951±40

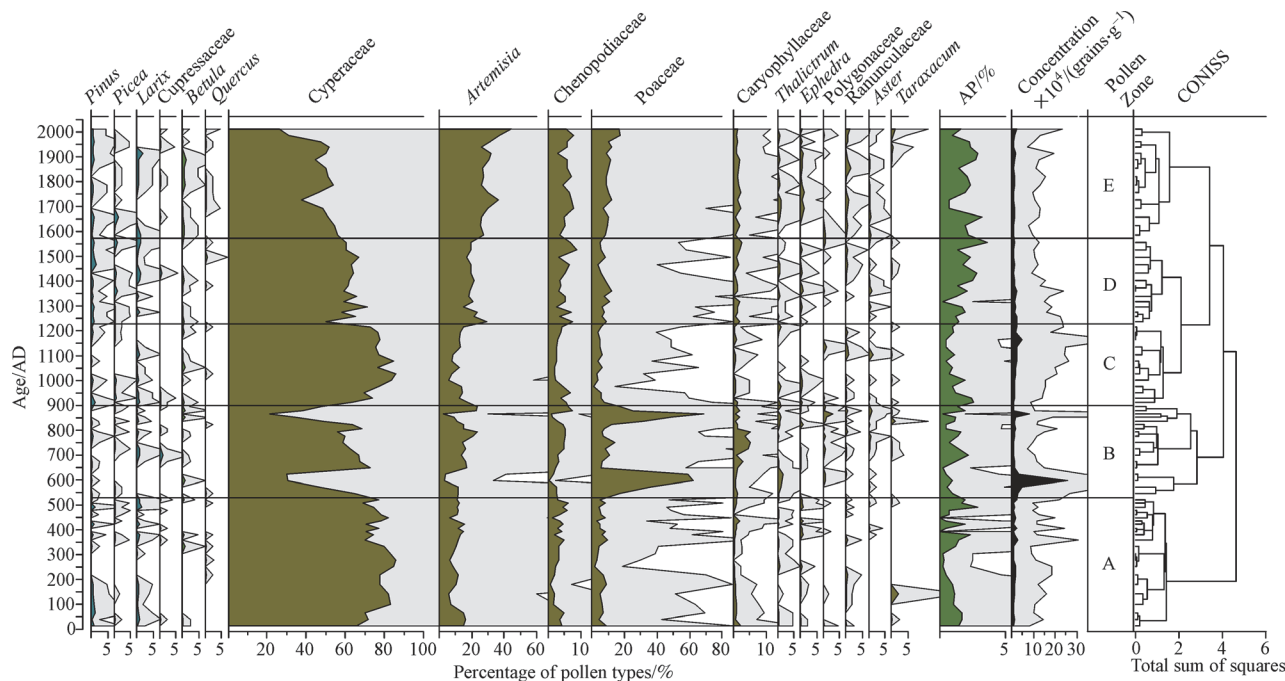


Fig. 3 Pollen data of YSKL peat core.

*Artemisia* (3.03%–44.65%), *Poaceae* (1.41%–68.75%), *Chenopodiaceae* (0.24%–8.91%) and *Caryophyllaceae* (0.23%–5.29%). Pollen concentrations ranged from  $7.42 \times 10^4$  to  $2.59 \times 10^6$  grains/g. The pollen assemblage of the YSKL core can be divided into five major zones, using the sequential cluster analysis (CONISS) (Fig. 3), listed as follows.

**Pollen zone A** (83–62 cm; 12–520 AD): The assemblage is dominated by NAP types. The percentages of *Cyperaceae*, *Artemisia*, *Poaceae* and *Chenopodiaceae* were 64.81%–84.99%, 6.67%–15.44%, 1.85%–9.81%, and 0.72%–6.16%, respectively. The content of AP was relatively low, with a mean of 1.06%, and it was dominated by *Pinus* (0.18%–1.21%) and *Larix* (0.24%–1.45%) in this interval. The *Caryophyllaceae* pollen percentage was 0.23%–2.13%.

**Pollen zone B** (61–43 cm; 520–900 AD): This assemblage is also dominated by NAP types. Compared to pollen zone A, even though the *Cyperaceae* pollen (33.1%–50.4%) was still dominant, it saw a slightly declining trend with a mean of 51.46%. Two pronounced features were observed: 1) a dramatic increase in the *Poaceae* pollen percentage (averagely 25.16%), with two higher values at 57–59 cm (~52.41%) and 39–42 cm (~43.58%), and 2) a slight increase in the *Caryophyllaceae* pollen, with a mean of 2.01%. No obvious change was observed in AP.

**Pollen zone C** (42–29 cm; 900–1230 AD): This zone is characterized by gradual increases in *Pinus* (averagely 0.28%), *Larix* (averagely 0.26%), and *Picea* (averagely 0.23%) pollen percentages. Similar to pollen zone A, the

*Cyperaceae* pollen predominated again with a mean of 74.50%. The averaged pollen percentages of *Artemisia*, *Chenopodiaceae*, *Poaceae*, and *Caryophyllaceae* are 12.85%, 3.77%, 5.73%, and 0.48%, respectively.

**Pollen zone D** (28–15 cm; 1230–1580 AD): In comparison with the underlying pollen zone C, the pollen percentages of *Artemisia* (averagely 20.32%), *Chenopodiaceae* (averagely 4.97%), *Poaceae* (averagely 7.65%), and *Caryophyllaceae* (averagely 1.15%) increased considerably at the expense of *Cyperaceae* pollen (averagely 61.59%). This zone is characterized by increases in the *Pinus* (averagely 0.57%), *Larix* (averagely 0.45%), and *Picea* (averagely 0.37%) pollen percentages.

**Pollen zone E** (14–1 cm; 1580–2017 AD): AP had the largest value in the pollen assemblages with a mean of 1.93%. Similar to pollen zone D, the *Artemisia* (averagely 30.79%), *Chenopodiaceae* (averagely 6.03%), *Poaceae* (averagely 11.04%), and *Caryophyllaceae* (averagely 1.38%) pollen increased continuously at the expense of the *Cyperaceae* pollen percentage (averagely 46.04%).

### 3.2 PCA analysis results of YSKL core

Figure 4 presents the PCA results based on 17 selected pollen types and the total samples. The first and second principal components capture 48.20% and 26.45%, respectively, altogether accounting for 74.65% of the total variance within fossil pollen assemblages. Four groups were observed among the 17 pollen types (Fig. 4): 1) *Poaceae*, *Polygonaceae*, and *Thalictrum*, 2) *Cyperaceae*, 3) *Larix*, *Cupressaceae*, *Ephedra*, *Pinus*,

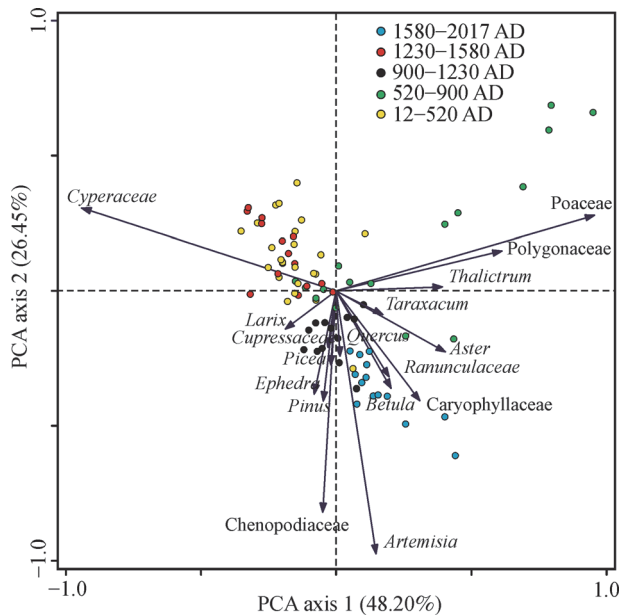


**Fig. 4** PCA ordination of principal 17 pollen taxa and samples from YSKL core.

*Picea*, and Chenopodiaceae, and 4) *Taraxacum*, *Aster*, *Quercus*, Ranunculaceae, *Betula*, Caryophyllaceae, and *Artemisia*. Hence, five clusters of samples well corresponded with the pollen assemblage zones, clearly separated from each other on the biplot of PCA scores along the first and the second axes: pollen zone A (12–520 AD) characterized by Cyperaceae, pollen zone B (520–900 AD) featuring Poaceae and Polygonaceae, pollen zone C (900–1230 AD) typified by Cyperaceae, *Artemisia*, *Pinus*, and *Larix*, and pollen zone D (1230–1580 AD) characterized by Cyperaceae, and pollen zone E (1580–2017 AD) featuring *Artemisia*, Caryophyllaceae, and *Betula*.

As shown in Fig. 4, the PCA axis 1 mainly separates Cyperaceae on the left from Poaceae on the right. Previous studies on pollen surface samples indicate that the primary sources of Cyperaceae pollen are wetlands and alpine meadows (Luo et al., 2010; Tian et al., 2013; Huang et al., 2015; Yu et al., 2017; Han et al., 2020). Moreover, modern pollen data also illustrate that, with rising elevation, Cyperaceae is more abundant than Poaceae (Huang et al., 2015). However, several Holocene pollen sequences inferred from the high-elevation peatlands of the Altai Mountains (Narenxia, Tuolehaite, and Halasazi Peatland) and other nearby sites (e.g., Lugovoe and Zhukovskoye Peatland) show that the relatively high contents of Cyperaceae pollen in the early Holocene corresponded with the warm-dry climate conditions and the relatively low contents in the late Holocene with the cold-wet climate conditions (Borisova et al., 2011; Blyakharchuk and Chernova, 2013; Feng et al., 2017; Huang et al., 2018; Wang and Zhang, 2019; Zhang et al., 2020b). It means that the high contents of Cyperaceae pollen might be an

indicator of warming climate in the Altai Mountains. Therefore, we consider that the PCA-1 scores and Cyperaceae/Poaceae (Cy/Po) ratios have a negative and positive correlation with the temperature, respectively. The PCA axis 2 mainly separates Cyperaceae and Poaceae above from Chenopodiaceae and *Artemisia* below (Fig. 4). Studies of modern pollen surface samples on drought-tolerance of different taxa in the nearby Tianshan Mountains suggest a pattern of Chenopodiaceae > *Artemisia* > Poaceae > Cyperaceae (Huang et al., 2015). Studies by Zheng et al. (2008) and Luo et al. (2010) suggest a similar pattern in arid and semi-arid China. Thus, the PCA-2 scores reflect the moisture changes, with the positive and negative values indicating wet and dry conditions, respectively.

## 4 Discussion

### 4.1 Climate change reflected by pollen data in YSKL Peatland

The vegetation and climate changes over the past 2000 years have been depicted by the pollen assemblages of the YSKL core. Specifically, in 12–520 AD, the vegetation was dominated by herbaceous plants with high abundance of Cyperaceae, Poaceae, *Artemisia*, and Chenopodiaceae (Fig. 3). The Cyperaceae pollen content was the highest in this interval, reflecting a relatively warm climate condition (Fig. 3). Furthermore, the PCA-1 score curve and Cy/Po ratios also imply a warmer climate interval (Figs. 5(c) and 5(d)). Additionally, the warm climate has been strongly supported by the reliable tree-ring-recorded summer temperature reconstruction in the Altai Mountains (Fig. 5(b); Büntgen et al., 2016). The PCA-2 score curve exhibited a wet climate interval, which is consistent with the *Sphagnum* carbon isotope ( $\delta^{13}\text{C}$ )-reconstructed high-moisture level (Yang et al., 2019a). The *Artemisia*/Chenopodiaceae (A/C) pollen ratios at the Bayan Nuur (site ⑦ in Fig. 1(a)) suggested a decreasing moisture trend (Fig. 5(g); Yang et al., 2019b). The SIB04 peat record from the southern Siberian Lowland (site ⑩ in Fig. 1(a)) exhibited a relatively shallow water table depth (Fig. 5(j); Wills et al., 2015).

From 520 AD to 900 AD, the Cyperaceae pollen content experienced two troughs, while the Poaceae content was marked by two peaks (Fig. 3). The increased scores of the PCA-1 axis and decreasing Cy/Po values suggest a low-temperature environment. Compared with the moisture trend in 12 AD–520 AD, the PCA-2 score displayed no obviously decreasing moisture. The  $\delta^{13}\text{C}$ -recorded moisture of the YSKL core and the A/C-indicated moisture record of the Bayan Nuur both suggest a wet environment (Yang et al., 2019a, 2019b). The water table reconstruction in the southern Siberian Lowland was very close to the peat surface (Wills et al., 2015). The reconstructed moisture

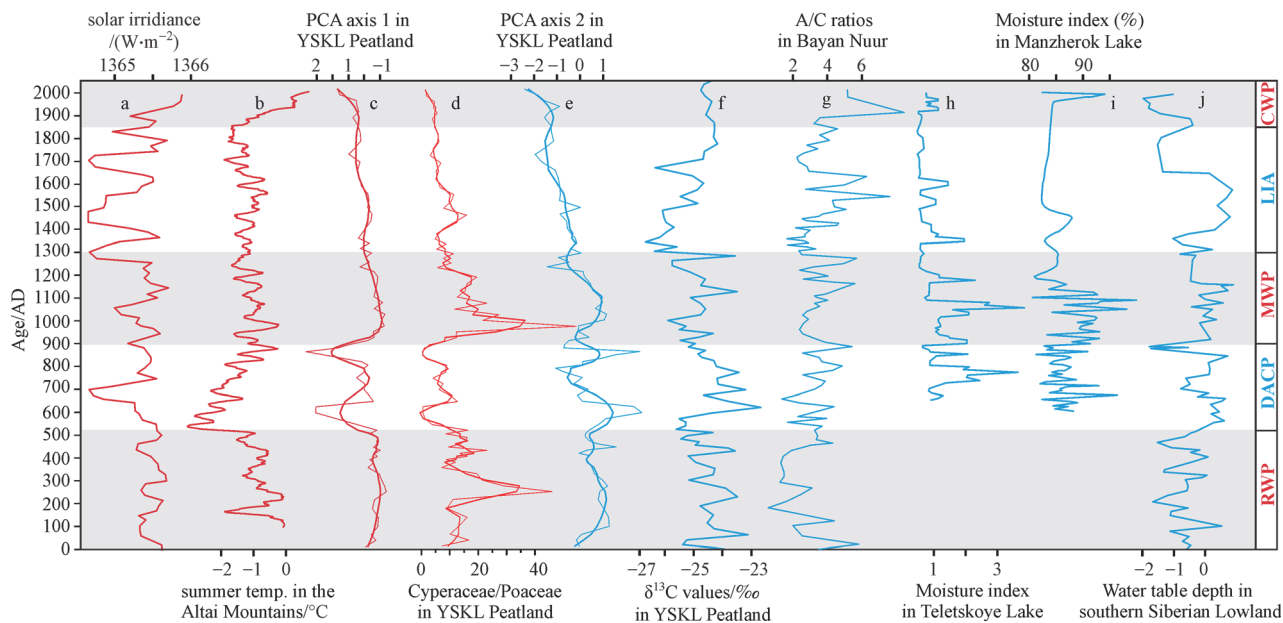


**Fig. 5** a: total solar irradiance (Steinhilber et al., 2009); b: tree-ring-recorded summer temperature reconstruction in the Altai Mountains (Büntgen et al., 2016); c: PCA axis 1 in YSKL Peatland (this study); d: Cyperaceae/Poaceae (Cy/Po) ratios in YSKL Peatland (this study); e: PCA axis 2 in YSKL Peatland (this study); f:  $\delta^{13}\text{C}_{\text{cellulose}}$ -indicated moisture in YSKL Peatland (Yang et al., 2019a); g: *Artemisia*/Chenopodiaceae (A/C) ratios in Bayan Nuur (Yang et al., 2019b); h: moisture index in Teletskoye Lake (Rudaya et al., 2012); i: moisture index in Manzherok Lake (Blyakharchuk et al., 2017); j: water table depth in southern Siberian Lowland (Wills et al., 2015). Note: RWP-Roman Warm Period, DACP-Dark Age Cold Period, MWP-Medieval Warm Period, LIA-Little Ice Age and CWP-Current Warm Period.

index based on pollen data from the Teletskoye Lake (site ⑧ in Fig. 1(a)) (Fig. 5(h), Rudaya et al., 2016) and Manzherok Lake (site ⑨ in Fig. 1(a)) (Fig. 5(i), Blyakharchuk et al., 2017) was also indicative of a wet climate.

Similar to the climate feature from 12 to 520 AD, the PCA-1 score curve and Cy/Po ratios exhibited a warmer climate between 900 and 1300 AD, while a similar wet climate was revealed by the high PCA-2 scores and the positive *Sphagnum*  $\delta^{13}\text{C}$  values (Yang et al., 2019a), which is supported by four moisture records from the Bayan Nuur (Yang et al., 2019b), Teletskoye Lake (Rudaya et al., 2016), Manzherok Lake (Blyakharchuk et al., 2017) and southern Siberian Lowland (Wills et al., 2015).

During 1300–1850 AD, the Cyperaceae pollen reduced gradually, while other herbaceous pollen contents (Poaceae, *Artemisia*, and Chenopodiaceae) increased apparently. The increased scores of the PCA-2 and decreased Cy/Po ratios marked a cooling climate trend, corresponding with the lower summer temperature found from tree-ring records in the Altai Mountains (Fig. 5(b); Büntgen et al., 2016). The lower PCA-2 score and the negative  $\delta^{13}\text{C}$  values still displayed a drying climatic condition. The lowest moisture index was found at the Teletskoye Lake (Rudaya et al., 2016) and Manzherok Lake (Blyakharchuk et al., 2017), whereas two moisture curves inferred from the Bayan Nuur and southern Siberian Lowland also showed a lowering moisture trend in this interval (Wills et al., 2015; Yang et al., 2019b).

The percentage of Cyperaceae pollen obviously reduced after 1850 AD, while the Poaceae, *Artemisia*, and Chenopodiaceae pollen increased. The AP content reached the highest level in the whole YSKL core. Neither the PCA-1 score curve nor the Cy/Po ratios suggested a warming climate (Fig. 5). The PCA-2 score curve denoted a relatively dry climatic condition, and other reconstructed moisture indices also reflected a dry environment (Rudaya et al., 2016; Wills et al., 2015; Blyakharchuk et al., 2017; Yang et al., 2019b). It should be noted that the  $\delta^{13}\text{C}$ -indicated a wet level after ~1900 AD, and that may be misleading because the measured materials for the carbon isotope were from *Carex*-dominated residuals (Yang et al., 2019a).

Overall, the pollen-based temperature curves (PCA-1 scores and Cy/Po ratios) at the YSKL Peat are strongly supported by the reliable tree-ring-based summer temperature sequence retrieved from the Russian Altai Mountains (Fig. 5(b); Büntgen et al., 2016). Their responses were sensitive to the solar irradiance-modulated temperature oscillations (Fig. 5(a)) in the Northern Hemisphere; these oscillations feature in five intervals, including the Roman Warm Period (RWP, 0–500 AD), Dark Age Cold Period (DACP, 500–900 AD), Medieval Warm Period (MWP, 900–1300 AD), Little Ice Age (LIA, 1300–1850 AD) and Current Warm Period (CWP, since 1850 AD) (Steinhilber et al., 2009; PAGES 2k Consortium, 2019). Combined with the moisture data from the Altai Mountains, the climate seems to indicate a warm-wet RWP, a cool-wet

DACP, a warm-wet MWP and a cool-dry LIA. In addition, the YSKL pollen data don't show a warming CWP, which may be attributed to the intensified disturbance of vegetation evolution by human activities in the Altai Mountains and the surrounding regions (Tian et al., 2014).

#### 4.2 Spatial differences of vegetation in the Altai Mountains over the past 2000 years

To investigate the spatial differences of vegetation along the NW-SE gradient in the Altai Mountains, the pollen assemblages of the YSKL Peatland in the past 2000 years were compared with other pollen sequences inferred from the Narenxia (NRX) Peatland (48.80°N, 86.90°E, 1760 m a.s.l.; Feng et al., 2017), Kanas (KN) Lake (48.72°N, 87.02°E, 1365 m a.s.l.; Huang et al., 2018), Big Black (BB) Peatland (48.68°N, 87.18°E, 2100 m a.s.l.; Xu et al., 2019), Tuolehaite (TLHT) Peatland (48.44°N, 87.54°E, 1700 m a.s.l.; Zhang et al., 2020b) and Halasazi (HLSZ) Peatland (48.12°N, 88.37°E, 2450 m a.s.l.; Zhang et al., 2020a) (sites ②–⑥ in Fig. 1(a)) along the NW-SE gradient in the Altai Mountains.

As shown in Fig. 6, a decreasing AP percentage was found along the NW-SE gradient in the Altai Mountains. Specifically, the AP percentage accounted for an average of 19.45% of the pollen sum in the NRX Peatland, 17.03% in the KN Lake, 12.73% in the BB Peatland, 8.49% in the TLHT Peatland, 4.53% in the HLSZ Peatland and 1.36% in the YSKL Peatland. The ratios of the predominant species (*Pinus*, *Picea*, *Betula*, and *Larix*) among the different areas in AP are as follows.

- NRX Peatland: 55.10%, 16.57%, 8.37%, and 7.38%
- KN Lake: 4.96%, 37.61%, 28.35%, and 25.41%
- BB Peatland: 26.00%, 11.69%, 38.46%, and 0.10%
- TLHT Peatland: 30.67%, 38.17%, 15.10%, and 7.30%
- HLSZ Peatland: 20.52%, 29.74%, 22.21%, and 10.21%
- YSKL Peatland: 33.51%, 27.11%, 23.06%, and 33.21%

Converse to the changeable trend of AP among these six records, their NAP percentages have an increasing trend along NW-SE gradient of the Altai Mountains (Fig. 6). These ratios of *Pinus*, *Picea*, *Betula*, and *Larix* pollen are mostly consistent with modern distributions of taiga forests and also reflect the NW-SE gradients of decreasing moisture and increasing climatic continentality seen in the Altai Mountains over the past 2000 years (Blyakharchuk et al., 2004, 2007).

Furthermore, we investigated the vegetation dynamics in the Altai Mountains across different climatic intervals for the past 2000 years (Fig. 5). During the warm-wet RWP, six pollen records showed that *Pinus* and *Picea* were the predominant trees with some *Betula* and *Larix* in the Altai Mountains. The *Larix* pollen content in KN Lake was higher than other sites. The herbaceous species mainly consisted of Cyperaceae, *Artemisia*, and Poaceae in the NRX, TLHT and YSKL Peatlands, while Chenopodiaceae,

*Artemisia*, and Poaceae were the dominant components in the KN Lake and HLSZ Peatland. During the DACP, the regional climate changed to extremely cold and wet conditions, and pollen assemblages exhibited an increase of *Pinus* and decrease of *Picea* and *Betula*. A substantial decrease of Cyperaceae content was presented in the NRX and YSKL Peatlands. The proportion of *Artemisia* increased at the expense of Chenopodiaceae during six sequences.

The climate turned to relatively warm and wet conditions during the MWP. The *Pinus* pollen which saw a decreasing trend before 1150 AD, was at a relatively high level afterwards. Slightly increased *Picea* content and decreased *Betula* proportions were observed in this interval, whereas increased contents of Cyperaceae, Chenopodiaceae, and Poaceae were also observed during the MWP. Climatic cooling and reduced moisture prevailed during the LIA. All pollen assemblages reflected an increasing content of *Pinus* and *Betula* with a reduction of *Picea* in this interval, while the proportion of *Artemisia* increased at the expense of Chenopodiaceae and Cyperaceae. Since 1850 AD, the increasing AP indicates forest regeneration (mainly *Picea* and *Pinus*) in the Altai Mountains. Additionally, the increased *Artemisia* and Poaceae pollen indicate rising moisture levels in the high-elevation Altai Mountains.

The analysis of vegetation dynamics over the past 2000 years shows different responses of pollen types to climate changes in the Altai Mountains. Specifically, the *Pinus* pollen percentage is negatively related with temperature variations, while the *Picea* pollen percentage is positively related. It is consistent with our previous study of the Holocene epoch (Zhang et al., 2020c), because *Pinus* is more cold-tolerant in comparison with *Picea* (Blyakharchuk and Chernova, 2013). The relatively high *Betula* content recorded in the KN Lake was because *Betula* forests widely grow at low elevations (Blyakharchuk and Chernova, 2013). The YSKL pollen data from the Altai Mountains reveal that the climate has been cooling and drying over the past 2000 years (Fig. 5), leading to the expansion of *Pinus* forests at the expense of *Picea* and *Betula* forests, and an increased abundance of *Artemisia*, Poaceae and Chenopodiaceae pollen at the expense of Cyperaceae pollen (Fig. 6). Therefore, we can propose that taiga (mainly *Pinus* forest) has slightly spread in the Altai Mountains over the past 2000 years. We can also propose that the steppe (*Artemisia*, Poaceae, and Chenopodiaceae) have significantly recovered, based on the fact that Cyperaceae is an essential component of the wetlands (Tian et al., 2013; Feng et al., 2017; Yu et al., 2017).

#### 4.3 The rise of Mongol Empire (1206–1260 AD)

Archaeological data show that the Eurasian Steppe Silk Road at 40°N–50°N connected the Central Asian and

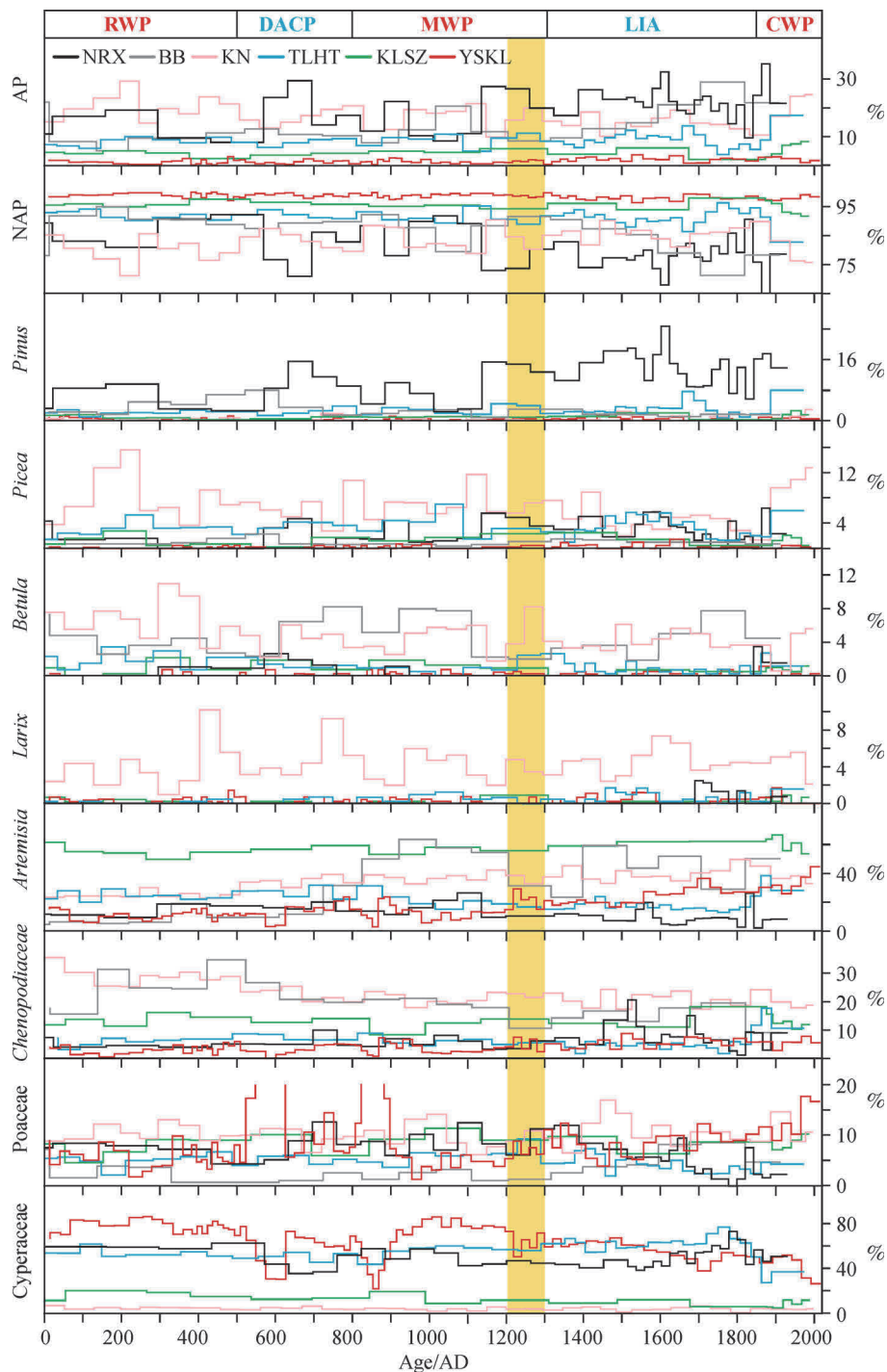


**Fig. 6** Percentages of arboreal pollen (AP) and non-arboreal pollen (NAP), selected main pollen proportions of *Pinus*, *Picea*, *Betula*, *Larix*, *Artemisia*, Chenopodiaceae, Poaceae and Cyperaceae in the Altai Mountains during the past 2000 years. Yellow belt indicates the Mongol Empire period.

Eastern European civilizations in the west with the East Asian civilization in the east (Golden, 1990; Alekseev et al., 2001). Climate change is the principal factor triggering the civilization's success along the Eurasian Steppe Silk Road (Blyakharchuk and Chernova, 2013; Pederson et al., 2014; Putnam et al., 2016; An et al., 2017; Zhou et al.,

2020). This steppe belt was a considerable influence in the formation of the Mongol Empire with the episodic spread of pastoralists from their Eurasian steppe homelands, all of which has been extensively discussed in recent decades. Huntington (1907) proposed that drought may have stimulated the Mongols' outward expansion, whereas

Jenkins (1974) reported that the climatic cooling was coeval with nomadic irruptions out of the Mongolian steppe. Pederson et al. (2014) proposed that the wet conditions stimulated the Mongol rise in the eventual Mongolian heartland, and more recently, Putnam et al. (2016) attributed the Mongol rise to the southward spreading of grazing land that helped fuel Mongol conquests across Eurasia in the face of the positive water balance of interior Asia under the impact of LIA climate.

In the Altai Mountains and the surrounding regions, the temperature- and moisture-related proxies indicate a relatively warm and wet climate condition during the Mongol period (Fig. 5). The YSKL pollen data regarding the increasing *Artemisa*, Chenopodiaceae, and Poaceae pollen in the Altai Mountains indicate the increased steppe biological yield and its expanded area during this interval (Fig. 3), which is supported by other pollen records in the nearby sites (Tian et al., 2013; Rudaya et al., 2016; Yang et al., 2019b). Therefore, we can propose that the warm-wet climate condition led to an increase in biomass and southward expansion of the steppe in arid regions, which may have powered the military conquests of the Mongol cavalry (Pederson et al., 2014; Putnam et al., 2016).

## 5 Conclusions

The YSKL pollen assemblages reveal the vegetation and climate changes over the past 2000 years in the south-eastern Altai Mountains. The results indicate that the climate was warm-wet for RWP, cold-wet for DACP, warm-wet for MWP, and cool-dry for LIA. Combined with other pollen data (NRX Peatland, BB Peatland, KN Lake, TLHT Peatland, and HLSZ Peatland), the AP percentage shows a decreasing trend along the NW-SE gradient of the Altai Mountains. As a whole, the coniferous taiga grew slightly, and the steppe recovered over the past 2000 years in the Altai Mountains.

**Acknowledgements** This research was financially supported by Western Young Scholar Program-B of Chinese Academy of Sciences (No. 2018-XBQNXZ-B-020), National Natural Science Foundation of China (Grant Nos. 41771234 and 41803024) and Open Fund of State Key Laboratory of Loess and Quaternary Geology (No. SKLLQG2011).

## References

- An C B, Wang W, Duan F T, Huang W, Chen F H (2017). Environmental changes and cultural exchange between East and West along the Silk Road in arid Central Asia. *Acta Geogr Sin*, 5: 875–891 (in Chinese)
- Alekseev A Y, Bokovenko N A, Boltrik Y, Chugunov K A, Cook G, Dergachev V A, Kovalyukh N, Possnert G, van der Plicht J, Scott E M, Sementsov A, Skripkin V, Vasiliev S, Zaitseva G (2001). A Chronology of the Scythian antiquities of Eurasia based on new archaeological and  $^{14}\text{C}$  data. *Radiocarbon*, 43(2B): 1085–1107
- Birks H J B, Gordon A D (1985). *Numerical Methods in Quaternary Analysis*. London: Academic Press
- Blaauw M (2010) Methods and code for ‘classical’ age-modelling of radiocarbon sequences. *Quat. Geochro.* 5 (5): 512–518
- Blyakharchuk T A, Wright H E, Borodavko P S, van der Knaap W O, Ammann B (2004). Late glacial and Holocene vegetation changes on the Ulagan high-mountains plateau, Altai Mountains, southern Siberia. *Palaeogeogr Palaeoclimatol Palaeoecol*, 209(1–4): 259–279
- Blyakharchuk T A, Wright H E, Borodavko P S, van der Knaap W O, Ammann B (2008). The role of pingos in the development of the Dzhangyskol lake-pingo complex, central Altai Mountains, southern Siberia. *Palaeogeogr Palaeoclimatol Palaeoecol*, 257(4): 404–420
- Blyakharchuk T A, Wright H E, Borodavko P S, van der Knaap W O, Ammann B (2007). Late glacial and Holocene vegetational history of the Altai Mountains (southwestern Tuva Republic, Siberia). *Palaeogeogr Palaeoclimatol Palaeoecol*, 245(3–4): 518–534
- Blyakharchuk T A, Chernova N A (2013). Vegetation and climate in the Western Sayan Mts according to pollen data from Lugovoe Mire as a background for prehistoric cultural change in southern Middle Siberia. *Quat Sci Rev*, 75: 22–42
- Blyakharchuk T, Eirikh A, Mitrofanova E, Li H C, Kang S C (2017). High resolution palaeoecological records for climatic and environmental changes during the last 1350 years from Manzherok Lake, western foothills of the Altai Mountains, Russia. *Quat Int*, 447: 59–74
- Borisov O (1957). *The Climate of Soviet Union* (translated by Sui TK). Beijing: Science Press (in Chinese)
- Borisova O K, Novenko E Y, Zelikson E M, Kremenetski K V (2011). Late glacial and Holocene vegetational and climatic changes in the southern taiga zone of West Siberia according to pollen records from Zhukovskoye peat mire. *Quat Int*, 237(1–2): 65–73
- Büntgen U, Myglan V S, Ljungqvist F C, McCormick M, Di Cosmo N, Sigl M, Jungclaus J, Wagner S, Krusic P J, Esper J, Kaplan O J, de Vaan M A C, Luterbacher J, Wacker L, Tegel W, Kirilyanov A V (2016). Cooling and societal change during the Late Antique Little Ice Age from 536 to around 660 AD. *Nat Geosci*, 9(3): 231–236
- Feng Z D, Sun A Z, Abdusalih N, Ran M, Kurban A, Lan B, Zhang D L, Yang Y P (2017). Vegetation changes and associated climatic changes in the southern Altai Mountains within China during the Holocene. *Holocene*, 27(5): 683–693
- Golden P B (1990). *The Peoples of the South Russian Steppes*. Cambridge: Cambridge University Press
- Han D X, Gao C Y, Liu H X, Yu X F, Li Y H, Cong J X, Wang G P (2020). Vegetation dynamics and its response to climate change during the past 2000 years along the Amur River Basin, Northeast China. *Ecol Indic*, 117: 106577
- Huang X Z, Chen C Z, Jia W N, An C B, Zhou A F, Zhang J W, Jin M, Xia D S, Chen F H, Grimm E C (2015). Vegetation and climate history reconstructed from an alpine lake in central Tianshan Mountains since 8.5 ka BP. *Palaeogeogr Palaeoclimatol Palaeoecol*, 432: 36–48
- Huang X Z, Peng W, Rudaya N, Grimm E C, Chen X M, Cao X Y, Zhang J, Pan X D, Liu S S, Chen C Z, Chen F H (2018). Holocene vegetation and climate dynamics in the Altai Mountains and surrounding areas. *Geophys Res Lett*, 45(13): 6628–6636
- Huntington E (1907). *Lop-Nor. A Chinese Lake. Part I. The Unexplored*

- Salt Desert of Lop. *Bull Am Geogr Soc*, 39(2): 65–77
- Jenkins G (1974). A note on climatic cycles and the rise of Chinggis Khan. *Central Asiatic Journal*, 18(4): 217–226
- Li Y, Zhang D, Andreeva M, Li Y, Fan L, Tang M (2020). Temporal-spatial variability of modern climate in the Altai Mountains during 1970–2015. *PLoS One*, 15(3): e0230196
- Luo C X, Zheng Z, Tarasov P, Nakagawa T, Pan A D, Xu Q H, Lu H Y, Huang K Y (2010). A potential of pollen-based climate reconstruction using a modern pollen-climate dataset from arid northern and western China. *Rev Palaeobot Palynol*, 160(3–4): 111–125
- Milkov F N, Gvozdezky N A (1996). *Natural Geography of the Soviet Union—A Brief Introduction to the Caucasus of the Soviet Union*. Beijing: Commercial Press
- PAGES 2k Consortium (2019). Consistent multidecadal variability in global temperature reconstructions and simulations over the Common Era. *Nature Geosci*, 12: 643–649
- Pederson N, Hessel A E, Baatarbileg N, Anchukaitis K J, Di Cosmo N (2014). Pluvials, droughts, the Mongol Empire, and modern Mongolia. *Proc Natl Acad Sci USA*, 111(12): 4375–4379
- Putnam A E, Putnam D E, Andreu-Hayles L, Cook E R, Palmer J G, Clark E H, Wang C, Chen F, Denton G H, Boyle D P, Bassett S D, Birkel S D, Martin-Fernandez J, Hajdas I, Southon J, Garner C B, Cheng H, Broecker W S (2016). Little Ice Age wetting of interior Asian deserts and the rise of the Mongol Empire. *Quat Sci Rev*, 131: 33–50
- Rudaya N, Tarasov P, Dorofeyuk N, Solovieva N, Kalugin I, Andreev A, Daryin A, Diekmann B, Riedel F, Tserendash N, Wagnere M (2009). Holocene environments and climate in the Mongolian Altai reconstructed from the Hoton-Nur pollen and diatom records, a step towards better understanding climate dynamics in Central Asia. *Quat Sci Rev*, 28(5–6): 540–554
- Rudaya N, Nazarova L, Novenko E, Andreev A, Kalugin I, Daryin A, Babich V, Li H C, Shilov P (2016). Quantitative reconstructions of mid- to late holocene climate and vegetation in the north-eastern altai mountains recorded in lake teletskoye. *Global Planet Change*, 141: 12–24
- Steinhilber F, Beer J, Fröhlich C (2009). Total solar irradiance during the Holocene. *Geophys Res Lett*, 36(19): L19704
- TerBraak C J F, Smilauer P (2003). *CANOCO Reference Manual and CanoDraw for Windows User's Guide: Software for Canonical Community Ordination (Version 4.5)*. Ithaca: Microcomputer Power
- Tian F, Herzsuh U, Dallmeyer A, Xu Q, Mischke S, Biskaborn B K (2013). Environmental variability in the monsoon–westerlies transition zone during the last 1200 years: lake sediment analyses from central Mongolia and supra-regional synthesis. *Quat Sci Rev*, 73: 31–47
- Tian F, Herzsuh U, Mischke S, Schlütz F (2014). What drives the recent intensified vegetation degradation in Mongolia—climate change or human activity? *Holocene*, 24(10): 1206–1215
- Wang F, Qia N F, Zhang Y L, Yang H Q (1995). *Pollen Flora of China*. Beijing: Science Press
- Wang W, Zhang D L (2019). Holocene vegetation evolution and climatic dynamics inferred from an ombrotrophic peat sequence in the southern Altai Mountains within China. *Global Planet Change*, 179: 10–22
- Willis K S, Beilman D, Booth R K, Amesbury M, Holmquist J, MacDonald G (2015). Peatland paleohydrology in southern West Siberian Lowlands: comparison of multiple testate amoeba transfer functions, sites, and *Sphagnum*  $\delta^{13}\text{C}$  values. *Holocene*, 25(9): 1425–1436
- Xu H, Zhou K E, Lan J, Zhang G, Zhou X (2019). Arid Central Asia saw mid-Holocene drought. *Geology*, 47(3): 255–258
- Yang Y P, Zhang D L, Lan B, Abdusalih N, Feng Z D (2019a). Peat  $\delta^{13}\text{C}_{\text{cellulose}}$ -signified moisture variations over the past ~2200 years in the southern Altai Mountains, northwestern China. *J Asian Earth Sci*, 174: 59–67
- Yang Y P, Zhang D L, Sun A, Wang W, Lan B, Feng Z D (2019b). Pollen-based reconstructions of vegetation and climate changes during the late Holocene in the southern Altai Mountains. *Holocene*, 29(9): 1450–1458
- Yu S H, Zheng Z, Kershaw P, Skrypnikova M, Huang K Y (2017). A late Holocene record of vegetation and fire from the Amur Basin, far-eastern Russia. *Quat Int*, 432: 79–92
- Zhang D, Yang Y, Lan B (2018). Climate variability in the northern and southern Altai Mountains during the past 50 years. *Sci Rep*, 8(1): 3238
- Zhang D L, Chen X, Li Y M, Zhang S R (2020a). Holocene vegetation dynamics of the Altai Mountains in the Arid Central Asia. *Palaeogeogr Palaeoclimatol Palaeoecol*, 550: 109744
- Zhang D, Chen X, Li Y, Ran M, Yang Y, Zhang S, Feng Z (2020b). Holocene moisture variations in the Arid Central Asia: new evidence from the southern Altai Mountains of China. *Sci Total Environ*, 735: 139545
- Zhang D L, Chen X, Li Y M, Wang W, Sun A Z, Yang Y P, Ran M, Feng Z D (2020c). Response of vegetation to Holocene evolution of westerlies in the Asian Central Arid Zone. *Quat Sci Rev*, 229: 106138
- Zhang Y, Ma X H, Liu X T, Tong C, Yang P (2018b). Preliminary study on morphology, development process and peat accumulation rate of palsas during the Altai Mountains, northern Xinjiang Uygur Autonomous Region, northwest China. *Quat Sci*, 38(5): 1221–1232 (in Chinese)
- Zheng Z, Huang K Y, Xu Q H, Lu H Y, Cheddadi R, Luo Y L, Beaudouin C, Luo C X, Zheng Y W, Li C H, Wei J H, Du C B (2008). Comparison of climatic threshold of geographical distribution between dominant plants and surface pollen in China. *Sci China Earth Sci*, 51(8): 1107–1120
- Zhou X, Yu J, Spengler R N, Shen H, Zhao K, Ge J, Bao Y, Liu J, Yang Q, Chen G, Weiming Jia P, Li X (2020). 5200-year-old cereal grains from the eastern Altai Mountains redate the trans-Eurasian crop exchange. *Nat Plants*, 6(2): 78–87